HNSJ Humanities & Natural Sciences Journal
ISSN: (e) 2709-0833
www.hnjournal.net

Peer-Reviewed Journal
Indexed at: NSP - SJIF
Impact Factor 2022 = 4.91

RESEARCH TITLE

Biosynthesis Silver Nanoparticles and Assessment of Antibacterial Activity Against to some type of pathogenic bacteria

Ban M.A Alani[1], Rawia Abdelgain Elobaid Mohammed[2] , Harakat Mohsin Roomy[3]

[1] College of Medicine, university of Fallujah, Iraq
[2] College of science, university of Sudan of science and technology, Sudan
[3] Department of physics, Ministry of Education, Baghdad, Iraq

HNSJ, 2024, 5(7); https://doi.org/10.53796/hnsj57/3

Published at 01/07/2024 **Accepted at 06/06/2024**

Abstract

The present study included green synthesis, characterization and evaluation of antibacterial properties of silver nanoparticles (AgNPs) synthesized by using the leaf extract of Moringa oleifera for different concertation (1,2,3,4,5M). UV-Visible, scanning electron microscopy (SEM), and atomic force microscopy (AFM) analyses were significant in elucidating the morphology and distribution of the samples. FTIR analysis revealed the synthesis of AgNPs via the interaction of several phytochemicals with the extract solution. All the permitted quantities of these phytochemicals had various functional groups. UV-vis spectroscopy confirmed the fabrication of AgNPs at **250–460 nm.** The color change from yellow to red then brown in aqueous solution, this is evidence of the formation of silver nanoparticles, The X-ray diffraction (XRD) patterns indicated that the nanoparticles that were produced were of high purity and had a crystal structure with cubic facets, known as a face-centered cubic (FCC) structure. Silver nanoparticles (AgNPs) have substantial antibacterial efficacy against both S. aureus and E. coli. Based on an analysis of many attributes, it can be concluded that E. coli bacterium exhibits a higher level of resistance compared to S. aureus bacteria

Key Words: Green synthesis; Silver Nanoparticles; Plasmon resonance; Antibacterial Activity

1-Introduction

Nanotechnology is a technology for manipulating and controlling a substance at the nanometer level which can be used in all the different scientific fields, such as physics, chemistry, biology, and material science engineering [1]. Because they are simpler to synthesis, metal nanoparticles are the most researched type of nanoparticle material. Furthermore, these materials can be used for a multitude of purposes, engineering, medicine, and the environment. They are classified based on the synthesis process used, which can be physical, chemical, and biological [2]. Chemical reactions produce nanoparticles that compromise the host's normal cells, as well as environmentally unfavorable byproducts that may damage the host's normal cells [3]. The biosynthetic method is less expensive, safer and more beneficial. Many metals are also used, including copper, zinc oxide, lead, silver, gold, and others. the silver nanoparticles are the most promising [4]. Nanoparticles are interesting minerals for research, especially in medical and health fields. Ag is harmful to cells and is a powerful antimicrobial. Because Ag ions react with macromolecules in the cell including proteins and deoxyribonucleic acid (DNA), they can destroy bacterial cell walls, hinder bacterial cell growth, and disturb cell metabolism [5]. There are numerous ways to synthesis Ag nanoparticles, one of which is chemical reduction. Chemical reduction techniques are frequently employed due to their affordability and ease of application [6]. Utilizing reducing chemicals, this technique lowers Ag salts. However, using of chemicals in the synthesis of Ag nanoparticles causes toxic compounds (reducing agents and organic solvents) to adsorb on the material's surface, which will adversely and harmfully affect how it is used. It is therefore preferable to choose environmentally friendly techniques [7]. The green synthesis technique depends on the source materials, such as plants and plant parts, bacteria, fungi, and other bio-based molecules proteins, vitamins, molecules, etc. [8]. Medical plants have occupied an essential role in the lives of people all over the world, starting with ancient Indian Ayurveda and traditional medicine. Apart from their nutritional properties [9]. Moringa leaves have medicinal properties as the plant extracts of these leaves have shown strong antioxidant and antibacterial properties against both Gram-positive and Gram-negative bacteria [10]. The problem of antibiotic-resistant bacterial strains is becoming increasingly widespread throughout the world. Resistance to third-generation antibiotics has emerged in some microorganisms [11]. discovered that AgNPs have dual antibacterial properties against a variety of microorganisms, including Salmonella typhi, Pseudomonas aeruginosa, Vibrio cholerae, Staphylococcus aureus, and Escherichia coli. There are two types of nanoparticles: organic and inorganic, according to [12]. The antibacterial mechanism of AgNPs is not fully understood, but several properties of their antimicrobial effect have been identified. Various bacterial cell structures can be affected by silver ions. These ions appear to cling mostly to the cytoplasmic membrane and cell wall by electrostatic attraction and affinity for sulfur proteins, which increases membrane permeability and also causes damage to these structures [13,14]. The present work evaluated the synergistic effects of AgNPs made with M. oleifera extracts prepared by bio-friendly method, to combat antibiotic-resistant S. aureus and E. coli strains. After studying the physical properties of nanosilver prepared using the biological method.

2- Materials and Methods

2-1 Preparation plant extract of M. oleifera leaf

Following collection and washing in double distilled water to remove any dust, moringa leaves were dried in a dark room for two weeks before being ground into a powder. After drying, 10 g of each sample was ground into powder using a mortar and pestle and blender, and then added to 100 mL of distilled water using a magnetic stirrer for 1 h at room

temperature. The mixtures were then stirred for an entire day on an orbital shaker. The filtrate is taken and then sterilized using 0.4 micrometer bacterial filters. and the clear solution is placed. In the dryer, at a temperature of 35 °C until the extract dries, then a weight of (1 gram) is taken from the dry extract, and the volume is added to 100 ml of distilled water as shown in Figure1.Thus, a stock solution with a concentration of 10,000 ppm is obtained, which is mixed with a magnetic mixer for 15 minutes until dissolution. Complete the extract and from this solution the rest is prepared concentration.

Figure 1 preparation processes of extract of M. oleifera leaf

2.2-Synthesis of silver nanoparticles

For preparation different ratios (1, 2, 3, 4, and 5) ml of silver nanoparticles (Ag NPs), a 1 mM silver nitrate ($AgNO_3$) solution with a capacity of 100 mL was prepared. Then, at room temperature (28.0 ± 2.0 °C), 5 ml of $AgNO_3$ solution add to 1 ml of M. oleifera, then reduce the mixed solution in 100 ml of distilled water. After that, the mixture was left overnight at 30°C on a magnetic stirrer rotating at 150 rpm. And then the plant extract, reduction of silver nitrate to silver nanoparticles, and color change from yellow to red then brown in aqueous solution. This preparation process is repeated for four stages of silver nitrate solutions (2, 3, 4, and 5), see fig. 2

Figure 1 The final extract of the solution of the nanoparticles at different concentration.

2.3 Preparation of concentration:

Silver nanoparticles are prepared by changing the ratio of silver nitrate to the aqueous plant extract. Where 10 ml of silver nitrate is taken and added to the best sample resulting from the previous stages with 1 ml of the aqueous extract of the plant, i.e. the ratio is 1:10. This process is repeated for other ratios: 2:10, 3:10, and 4:10. After that, using the four tests, four images are obtained for each test and the best sample is taken to be used in killing or treating the two types of bacteria used in this project.

2.4Testing of the bacteria inhibitory

The inhibitory effectiveness of bacteria was tested on two types of bacteria, namely Staphylococcus aureus and Escherichia coli, where bacterial isolation was provided using the well diffusion method. The Ag NPs efect on bacteria was tested with a 100% solution as a synthesized AgNPs at the optimal conditions as a stock solution, and two different dilutions from the stock (50%,75%), and they were labeled as S50, S75 S100 After inoculating the bacterial cells on Petri dishes, the holes were made in the bacterial dishes and flled with diferent concentrations of synthesized Ag NPs. The plates were left at room temperature for a while, then incubated at 37 degrees Celsius for (18-24) hours, after which the inhibition zone around the holes was measured in millimeters antibacterial activities of Ag NPs samples were determined by measuring the inhibition zones around the samples.

2-4 Characterization of silver nanoparticles

A Japanese-made SHIMADZUUV-2600 UV-Vis spectrometer was used to record the absorbance spectrum (200–700 nm) of the synthesized silver nanoparticles. The phase purity of synthesized silver nanoparticles was determined using (SHIMADZU Japan) 40 kV. Current: 30 mA. Speed: 8 deg/min. Range: 10^{o} - 80^{o}). FTIR spectroscopy provides information on the functional groups present in nanoparticles, enabling us to determine the transformation of silver nanoparticles from the inorganic compound $AgNO_3$ to elemental silver. The spectra were scanned at a resolution of 4 cm^{-1} throughout the range of 4000–600 cm^{-1}. To carefully examine the very fine topography a field emission scanning electron microscope (FESEM) instrument was used.

4. Results and discussion

Figure 3 shows the UV absorption spectra of colloidal silver nanoparticles at various concentrations (1, 2, 3, 4, and 5) mol for silver nanoparticles (Ag NPs) synthesized using M. oleifera. AgNO3 molar concentration of 1 M shows homogeneous narrow absorption band at 270 nm with little variation in shift across different concentrations, this indicates the presence of Ag NPs in all sample of the plant extracts. This suggests that certain chemical compounds found in various regions of plants, at varying levels, may interact with the Ag NPs that are created. This leads to variations in the absorption qualities of the surface resonance. According to Figure 3, the sample containing 4 mol of AgNO3 was determined to be the most optimal. The absorbance peak exhibited a strong surface Plasmon resonance (SPR) at around 460 nm, indicating the successful production of Ag NPs. The earlier study [15] confirmed that the generation of AgNPs is supported by the surface plasmon resonance maxima, which ranges from 270 to 500 nm. At wavelength more than 500 nm, the absorbance curve gradually drops until it saturates and no absorption is observed. The quantum size effect has been shown to cause noticeable differences in absorption spectra. The results are consistent with thosereported by[16]

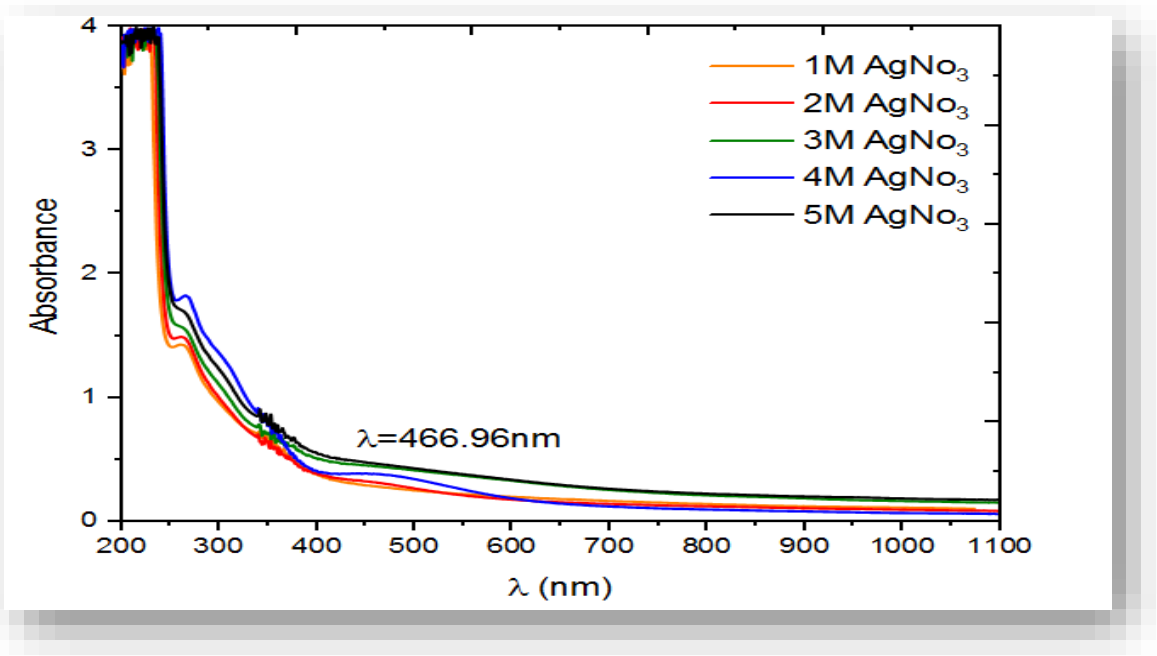

Figure 3 UV-visible absorption peak of M .oliefera synthesized silver nanoparticles at different concentration

Figure 4 exhibits the experimental X-ray diffraction (XRD) patterns of the Ag NP nanocomposites at various molarities of $AgNO_3$ (1, 2, 3, 4, and 5) mol. In the XRD pattern, four distinct peaks were observed at 2θ 37.935°, 44.139°, 64.349°, and 77.355° are the angles of crystal planes (111), (200), (220), and (311) respectively Bragg's reflections of the face-centered cubic (FCC) structure of metallic silver, respectively. No further peaks were seen from other crystal faces, suggesting a synthesis of FCC nanoparticles without impurities, thereby validating the purity of the produced material [17]. Based on the data presented in Figure 4 and Table 1, it is observed that the level of crystallization decreases as the molarities increase from 1 to 3 (69.244 to 53.036 nm). However, it then increases to 68.255 nm for the sample with 4 moles, indicating the highest degree of crystallization. Subsequently, the crystalline decreases again to 59.562 nm for the sample with 5 moles. The rationale for the impact of the Moringa oleifera plant's aqueous extract and its interaction with the nitrate solution might be attributed to [18].

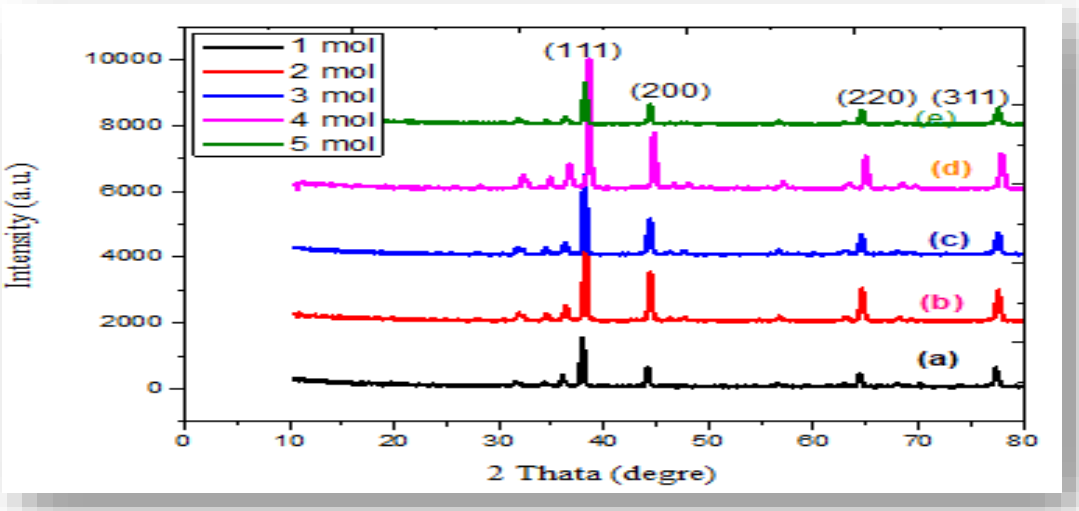

Figure 4 XRD patterns of for various molarty of $AgNO_3$.

Table 1 The stricture parameter of AgNPs with M. oliefera extracts

Samples $AgNO_3$ mol	2θ	d(exp.)	FWHM	I/Io.	D (nm)	Lattice constant
1	37.935	2.369	0.281	100	35.840	(111)
	44.139	2.050	0.323	23	34.262	(200)
	64.349	1.446	0.33	27	55.552	(220)
	77.355	1.232	0.23	30	151.322	(311)
Crystalline size average (nm)					69.244	
2	36.357	2.469	0.38	100	25.956	(111)
	44.397	2.038	0.276	26	40.273	(200)
	64.578	1.442	0.47	15	40.186	(220)
	77.530	1.23	0.31	17.6	118.32	(311)
Crystalline size average (nm)					56.183	
3	36.284	2.473	0.40	100	24.635	(111)
	44.34	2.041	0.393	10	37.9	(200)
	64.5	1.443	0.33	8.2	55.85	(220)
	77.49	1.230	0.39	7	93.761	(311)
Crystalline size average (nm)					53.036	
4	36.696	2.447	0.41	100	26.32	(111)
	44.760	2.023	0.291	10	38.43	(200)
	64.934	1.343	0.325	16.4	57.63	(220)
	77.91	1.225	0.251	12	150.64	(311)
Crystalline size average (nm)					68.255	
5	36.329	2.470	0.45	100	18.25	(111)
	44.361	2.040	0.314	28	35.378	(200)
	64.533	1.442	0.28	16	65.922	(220)
	77.570	1.23	0.31	17	118.70	(311)
Crystalline size average (nm)					59.562	

Figure 5 illustrates the dimensions, configurations, and structures of AgNPs synthesized by M. oliefera at various concentrations of $AgNO_3$ (1, 2, 3, 4, and 5). The FESEM pictures of AgNPs exhibit a diverse range of forms, providing evidence of their crystalline nature. The particle size values obtained from the FESEM image exhibit a random distribution, which may lead to the formation of unmanageable conglomerates in the presence of nanomaterials. The findings indicate that the particle sizes of the chosen samples were around 60.71 nm, 171.96 nm, 49.36 nm, 18.73 nm, and 105.22 nm. Clumping occurred, and the pictures exhibited excellent dispersion. Although the nanoparticles were crystalline, the AgNPs obtained from plants exhibited a diverse range of morphologies. The morphology of AgNPs might have been altered as a result of using diverse solvents or varying amounts of silver nitrate during their synthesis. Das et al. (2020) [19, 20] suggest that agglomeration may alter the morphology of nanoparticles. This aligns with their idea.

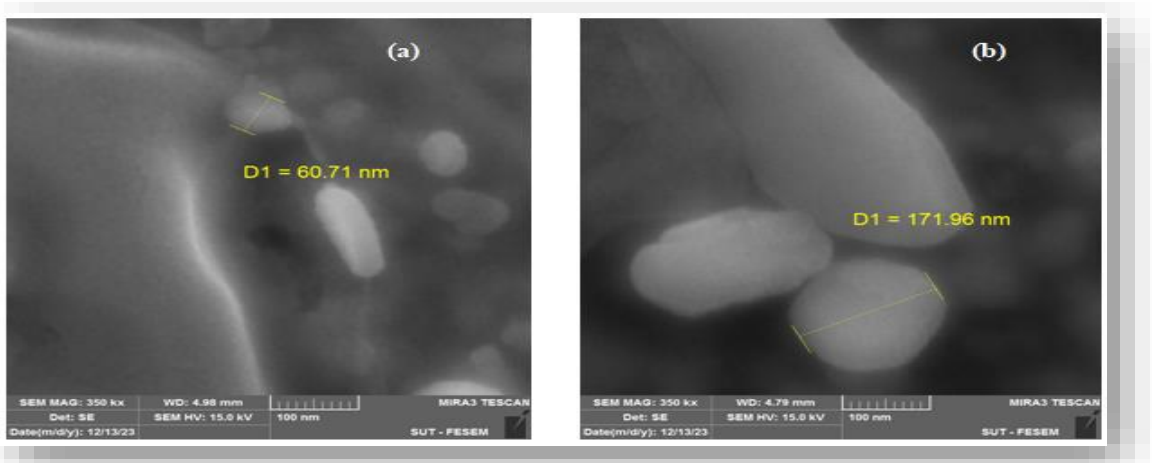

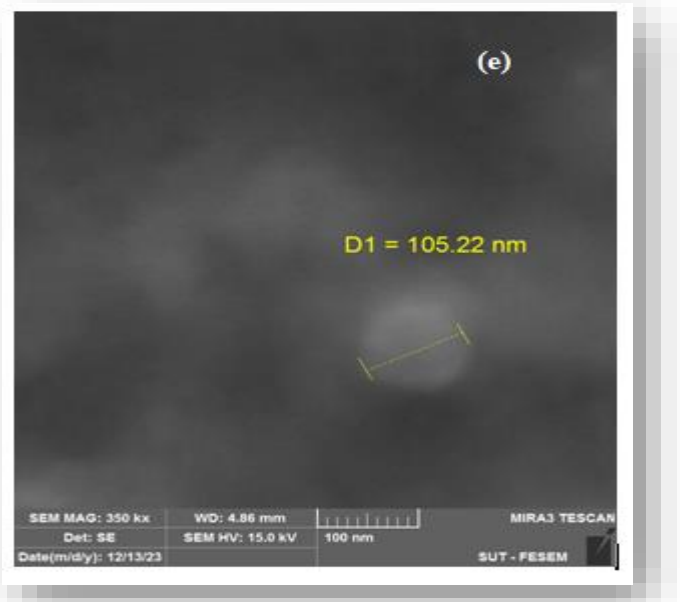

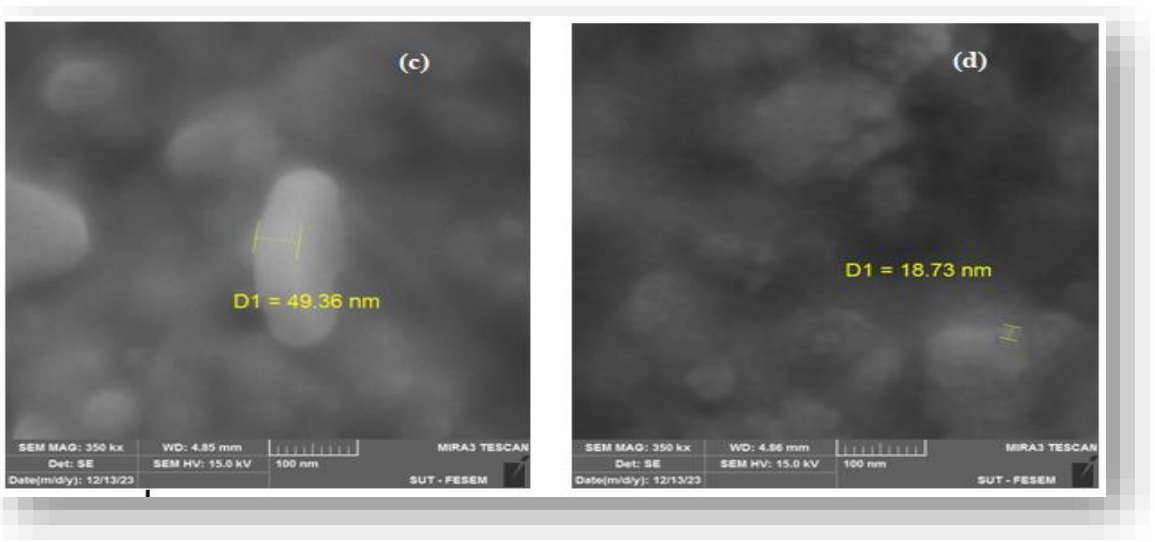

Figure 5 .SEM images of AgNPs with M. oleifera at different $AgNO_3$concentration (a)1 mol (b)2 mol (c) 3 mol, (d) 4 mol, (e)5 mol.

(Figure 6) confirms that the AgNPs produced are mostly composed of silver nanoparticles. Whereas, according to the energy dispersive X-ray (EDX) result, most of the major components showed intense peaks of Ag (78.23%) at 3.0 keV and O (21. 77%).These components likely play a role in stabilizing plant extracts and encapsulating biomolecules; In addition, they may be related to components found in plant proteins

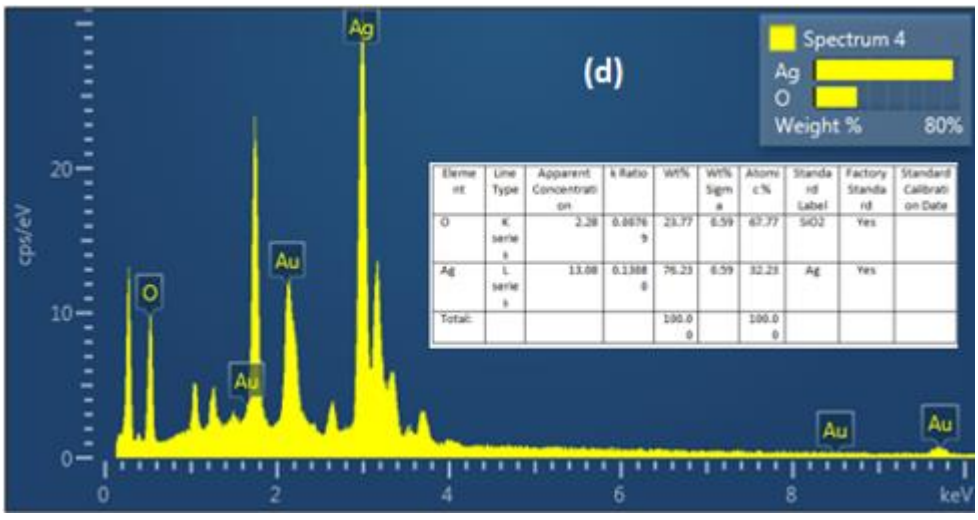

Figure 6. Energy dispersive x-ray (EDX) analysis of AgNPs with M. oleifera extracts at ratio (4mol)

Figure 7, we conducted FTIR analysis on $AgNO_3$ solutions with concentrations 4 mol as optimal concertation. Functional groups have been seen in the 500–4000 cm-1 range. As shown in the figure, 3417.85, 1375.25, 823.6, 800.46 cm-1. are notable peaks for the spectrum. The peaks at 3415.is attributed to the stretching vibrations of the hydroxyl (OH) functional group in alcohols compounds. The peaks at 1616.35, 1381.03, 1375.25, and 1379.10 cm-1 may be attributed to the presence of Protein I NNRnyl II (C=O) amides. The stretching observed at the peaks 630, 823.6, 800.45, and 800.46 cm-1, namely in the C-O region, might perhaps be attributed to the binding of an ether compound [20]. Based on the FTIR data, the peaks seen during the festivities suggest the existence of functional groups including hydroxyl, carbonyl, and ether linkages. These chemical substances may be classified as phytochemicals, as shown by Moodley et al. (2018).

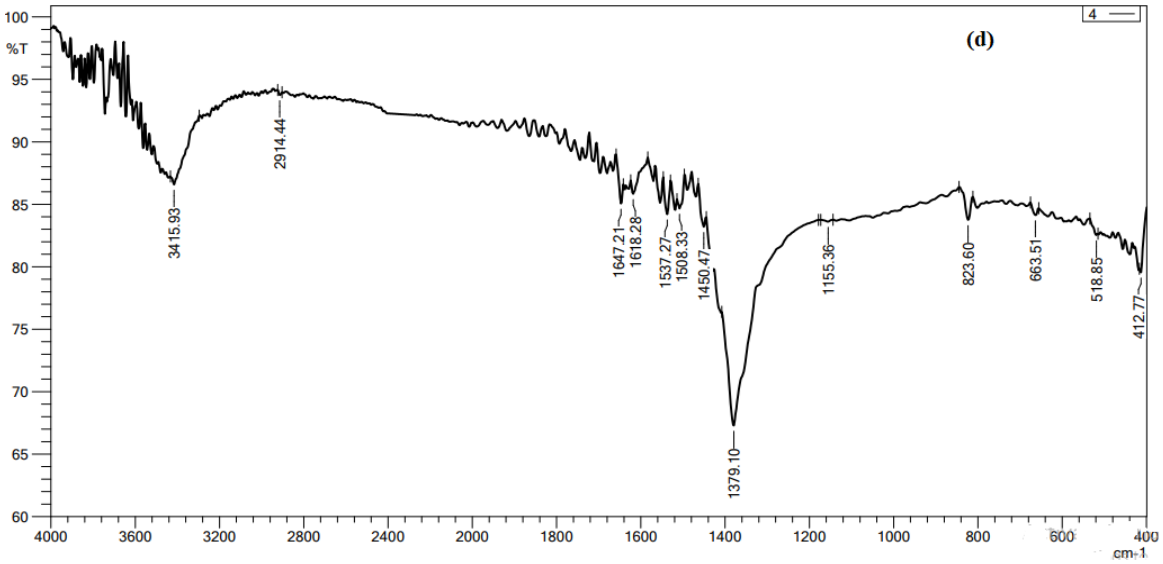

Figure 7 FTIR spectroscopy analysis of $AgNO_3$ with concentrations 4 mol,

Antimicrobial Activity:

The effect of Ag NPs obtained from M. oleifera at different concentrations (50,75, 100%) on inhibiting the growth of bacteria was studied for both type Gram-negative (Escherichia coli (ATCC 33849)) and Gram-positive (Staphylococcus aureus (ATCC 25923)) as in figures 8 and table 1. for first type Gram-negative (Escherichia coli), The figures and the table showed the inhibitory zone findings of Ag NPs combined with certain ratios of M. oleifera aqueous extract against E. coli bacteria. The table displays the concentrations achieved for each mixing ratio, which were pure plant extracts, 50%, 75%, and 100%. The size of the inhibitory zone increased as the concentration and mixing ratio of AgNP particles increased. The measurements for the sample were as follows: for pure plant extracts the results ranged 11.5 to 12.5, for 50% of the sample, the results ranged from 15 to 16.5 mm, for 75% of the sample, the results ranged from 16 to 17 mm, for 100% of the sample, the results ranged from 16 to 17.5 mm. On other hand, fore second type of (Staphylococcus aureus) ,the figures 9 and Table 2 displays The size of the inhibitory zone increased as the concentration and mixing ratios of AgNP particles increased. The measurements for the sample were as follows: for pure plant extracts the results ranged 13 to 14, for 50% of the sample, the results ranged from 16 to 18.5 mm, for 75% of the sample, the results ranged from 17.5 to 19 mm; and for 100% of the sample, the results ranged from 18 to 19 mm. The area of inhibition increased as the concentrations became larger, which aligns with the results reported by Chikara et al. (2021)[21]. The study found that Staphylococcus aureus is more sensitive to Ag NPs than E. coli. According to his explanation, the observed results could be attributed to the fact that Ag+ has a greater ability to degrade the cell wall of Gram-positive bacteria due to its single layer of peptidoglycan. In contrast, the dense peptidoglycan layer on the cell wall of Gram-negative bacteria acts as a barrier to prevent Ag+ ions from entering the cytoplasm.

Test Organisms	**Zone of inhibition (mm) ± SE of each concentration**							
	1:10		2:10		3:10		4:10	
E. coil	Conc. %	Inhibition zone (mm)	Conc.%	Inhibition zone (mm)	Con. %	Inhibition zone(mm)	Con. %	Inhibition zone (mm)
	pure	11.5		12		12		12.5

	plant extracts							
	50%	15	50%	15	50%	15.5	50%	16.5
	75%	16	75%	16.5	75%	16.5	75%	17
	100%	16	100%	16.5	100%	16.5	100%	17.5
S. aureus	pure plant extracts	13		13		13.5		14
	50%	16	50%	17.5	50%	17.5	50%	18.5
	75%	17.5	75%	18	75%	18	75%	19
	100%	18	100%	18	100%	18	100%	19

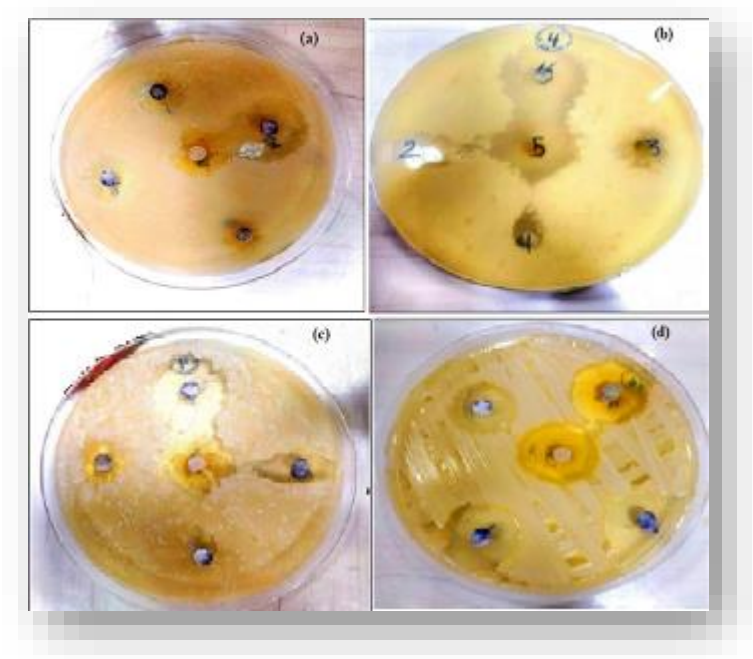

Figure 8 The zoom inhibition of AgNPs with M. oleifera against staphylococcus aureus (a) 1:10 cncentration (b) 2:10 cncentration, (c) 3:10 cncentration (d) 4:10 cncentration .

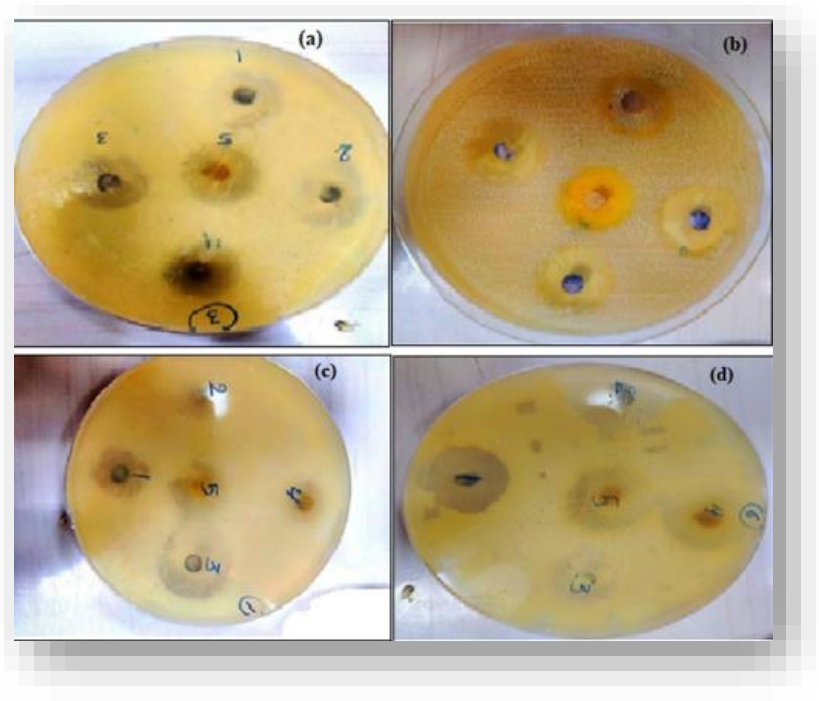

Figure 9 The zoom inhibition of AgNPs with M. oleifera against E. coli (a) 1:10 cncentration (b) 2:10 cncentration, (c) 3:10 cncentration (d) 4:10 cncentration

Reference

[1] Abbas,N.K., Al-Ogaidi, I. and Alsalmani ,M.(2017)'microwave-assisted synthesis of ZnS&ZnS-Ag nanoparticles and its antibacterial activity',GJBB. , 6 (4),pp. 677-682.

[2] Otávio Augusto L. dos Santos 1, Bianca Pizzorno Backx , Rasha A. Abumousa 3 and Mohamed Bououdina ,Environmental Implications Associated with the Development of Nanotechnology: From Synthesis to Disposal, Nanomaterials 2022, 12, 4319

[3] Das, B., Dash, K. S., Mandal, D., Ghosh, T., Chattopadhay, S., Tripathy, S., Dey, K. S. & Roy, S. 2017. Green synthesized silver nanoparticles destroy multidrug resistant 69 bacteria via reactive oxygen species mediated membrane damage. Arabian J. of Chemistry, 10, pp. 862–876.

[4] Anita Dhaka, Suresh Chand Mali, Sheetal Sharma, Rohini Trivedi, A review on biological synthesis of silver nanoparticles and their potential applications, Results in Chemistry Volume 6, December 2023, 101108.

[5] Siya Kamat and Madhuree Kumari, Emergence of microbial resistance against nanoparticles: Mechanisms and strategies Front Microbiol, 2023; 14: 1102615.

[6] A. Zielińska, E. Skwarek, A. Zaleska, M. Gazda, and J. Hupka, "Preparation of silver nanoparticles with controlled particles size," Procedia Chemistry, vol. 1, no. 2, pp. 1560–1566, 2009.

[7] A. Singh, D. Jain, M. K. Upadhyay, N. Khandelwal, and D. H. N. Verma, "Green synthesis of silver nanoparticles using Argenone mexicana leaf extract and their charactrization," Digest Journal of Nanomaterials and Biostructures, vol. 6, no. 1, pp. 483–489, 2010.

[8] Gorai ,S.(2011),' Bio-based Synthesis and Applications of SnO2 Nanoparticles-An Overview', J Mater Environ Sci.,9,pp.2894– 903.

[9]Moodley, S. J., Krishna, S. B. K., Pillay, K. &Govender, P. 2018. Green synthesis of silver nanoparticles from Moringaoleifera leaf extracts and its antimicrobial potential. Adv. Nat. Sci.: Nanosci. Nanotechnol., 9, pp. 1-10.

[10] Mmabatho Kgongoane Segwatibe, Sekelwa Cosa, and Kokoette Bassey, Antioxidant and Antimicrobial Evaluations of Moringa oleifera Lam Leaves Extract and Isolated Compounds, Molecules. 2023 Jan; 28(2): 899.

[11[1] Pal, N., &Agrawal, S. (2024). DRUMSTICK TREE (Moringaoleifera) Lam. LEAF EXTRACT MEDIATED SYNTHESIS OF SILVER NANOPARTICLES AND THEIR ANTIBACTERIAL ACTIVITY AGAINST NOSOCOMIAL BACTERIAL PATHOGENS. Journal of microbiology, biotechnology and food sciences, 13(4), e6015-e6015

[12] Nahar, K., Aziz, S., Bashar, S. M., Haque, A. & Al-Reza, S. 2020. Synthesis and characterization of Silver nanoparticles from Cinnamomumtamala leaf extract and its antibacterial potential. Int. J. Nano Dimens., 11 (1), pp. 88-98.

[13] Radzig MA, Nadtochenko VA, Koksharova OA, Kiwi J,Lipasova VA, Khmel IA. Antibacterial effects of silvernanoparticles on gram-negative bacteria: influence on thegrowth and biofilms formation, mechanisms of action.Colloids Surf B 2013;102:300–6.

[14] Hendiani, S., Abdi, A.A., Mohammadi, P. & Kharrazi, S. 2015. Synthesis of silver nanoparticles and its synergistic effects in combination with imipenem and two biocides against biofilm producing Acinetobacterbaumannii.Nanomedicine Journal, 2(3), pp. 291-298.

[15] Singh, C., Kumar, J. Kumar, P., Chauhan, S. B., Tiwari, N. K., Mishra, S. K., Srikrishna, S. Saini, R., Nath, G. & Singh, J. 2019. Green synthesis of silver nanoparticles using aqueous leaf extract of Premna integrifolia (L.) rich in polyphenols and evaluation of their antioxidant, antibacterial and cytotoxic activity. Biotechnology & biotechnological equipment, 33(1), pp. 359-371

[16] Mamdooh, N. W., & Naeem, G. A. (2022, July). The effect of temperature on green synthesis of silver nanoparticles. In AIP Conference Proceedings (Vol. 2450, No. 1). AIP Publishing.

[17] Mohsen, E., El-Borady, O. M., Mohamed, M. B., & Fahim, I. S. (2020). Synthesis and characterization of ciprofloxacin loaded silver nanoparticles and investigation of their antibacterial effect. Journal of Radiation Research and Applied Sciences, 13(1), 416-425.

[18] [154] Meng, Y. (2015). A sustainable approach to fabricating Ag nanoparticles /PVA hybrid nanofiber and its catalytic activity. Nanomaterials, 5(2), 1124-1135.

[19] Das, E. P, Abu-Yousef, A. I., Majdalawieh, F. A., Narasimhan, S. & Poltronieri, P. 2020. Green synthesis of encapsulated copper nanoparticles using a hydro alcoholic extract of Moringa oleifera leaves and assessment of their antioxidant and antimicrobial activities. Molecules, 25 (555), pp. 1-17

[20] Chhikara, N., Kaur, A., Mann, S., Garg, M. K., Sofi, S. A., & Panghal, A. (2021). Bioactive compounds, associated health benefits and safety considerations of Moringa oleifera L.: An updated review. Nutrition & Food Science, 51(2), 255-277.

[21] Niluxsshun, M. C. D., Masilamani, K. & Mathiventhan, U. 2021. Green synthesis of silver nanoparticles from the extracts of fruit peel of Citrus tangerina, 149 Citrus sinensis, and Citrus limon for antibacterial Activities. Bioinorganic Chemistry and Applications, pp.1-8. doi.org/10.1155/2021/6695734.